Ternary Blend Solar Cells Based on a Conjugated Polymer With Diketopyrrolopyrrole and Carbazole Units

AUTHOR(S):

Wang, Yanbin; Chen, Jinxing; Kim, Do Hyung; Wang, Biaobing; Iriguchi, Ryo; Ohkita, Hideo

CITATION:

Wang, Yanbin ...[et al]. Ternary Blend Solar Cells Based on a Conjugated Polymer With Diketopyrrolopyrrole and Carbazole Units. Frontiers in Energy Research 2018, 6: 113.

ISSUE DATE:

2018-10-24

URL:

http://hdl.handle.net/2433/234789

frontiers in Energy Research

ORIGINAL RESEARCH
published: 24 October 2018
doi: 10.3389/fenrg.2018.00113

Ternary Blend Solar Cells Based on a Conjugated Polymer With Diketopyrrolopyrrole and Carbazole Units

Yanbin Wang[1], Jinxing Chen[1], Hyung Do Kim[2], Biaobing Wang[1]*, Ryo Iriguchi[2] and Hideo Ohkita[2]**

[1] Jiangsu Key Laboratory of Environmentally Friendly Polymeric Materials, Jiangsu Collaborative Innovation Center of Photovolatic Science and Engineering, School of Materials Science and Engineering, Changzhou University, Changzhou, China, [2] Department of Polymer Chemistry, Graduate School of Engineering, Kyoto University, Kyoto, Japan

OPEN ACCESS

Edited by:
Itaru Osaka,
Hiroshima University, Japan

Reviewed by:
Letian Dou,
Purdue University, United States
Myungkwan Song,
Korea Institute of Materials Science, South Korea

***Correspondence:**
Yanbin Wang
wangyanbin@cczu.edu.cn
Biaobing Wang
biaobing@cczu.edu.cn
Hideo Ohkita
ohkita@photo.polym.kyoto-u.ac.jp

Specialty section:
This article was submitted to Solar Energy, a section of the journal Frontiers in Energy Research

Received: *27 July 2018*
Accepted: *04 October 2018*
Published: *24 October 2018*

Citation:
Wang Y, Chen J, Kim HD, Wang B, Iriguchi R and Ohkita H (2018) Ternary Blend Solar Cells Based on a Conjugated Polymer With Diketopyrrolopyrrole and Carbazole Units. Front. Energy Res. 6:113. doi: 10.3389/fenrg.2018.00113

Herein, we have synthesized a low-bandgap polymer (PCDPP4T) consisting of diketopyrrolopyrrole (DPP) and carbazole (Cz) units in the main chain. The absorption coefficient is as high as 1.3×10^5 cm^{-1} for PCDPP4T, which is slightly higher than 1.0×10^5 cm^{-1} for the monomer model compound (DPP4T-Cz). For ternary blend solar cells based on poly(3-hexylthiophene) (P3HT), [6,6]-phenyl-C_{61}-butyric acid methyl ester (PCBM), and only 3.4 wt% of PCDPP4T, the photocurrent increased and thus the power conversion efficiency (PCE) was improved by 30% relative to those of P3HT/PCBM binary reference cells. The improved photocurrent was ascribed partly to a complementary absorption of PCDPP4T in the near-infrared (near-IR) region, and partly to an efficient energy transfer from P3HT to PCDPP4T. We also discuss the origin for the improved photocurrent and requirements for further improvements.

Keywords: polymer solar cells, ternary blend, low-bandgap, diketopyrrolopyrrole, carbazole

INTRODUCTION

Polymer solar cells based on donor and acceptor binary blends have been widely studied in the past three decades (Halls et al., 1995; Yu et al., 1995; Shaheen et al., 2001; Padinger et al., 2003; Li et al., 2005, 2016; Kim et al., 2006; Peet et al., 2007; Liang et al., 2010; Dou et al., 2011; Liu et al., 2014; Vohra et al., 2015; Bin et al., 2016). In this period, the efficiency has been steadily improved every year. Currently, more than 13% has been reported (Zhao W. et al., 2017; Sun et al., 2018; Xu et al., 2018; Zhang S. et al., 2018). Nonetheless, it is not enough high compared to that of silicon-based solar cells. This is most probably because the photoactive layer cannot absorb whole of the solar light, which limits the short-circuit current density (J_{SC}) and hence the efficiency as well. To solve this issue, ternary blend solar cells have been proposed. By using three materials with complementary absorption bands, the optical response range can be easily expanded (Peet et al., 2008; Honda et al., 2009, 2010, 2011a; Ameri et al., 2012, 2013; Xu et al., 2013; Yang et al., 2013, 2015, 2017; Wang et al., 2014b,c, 2015a, 2018a,b; Lu et al., 2015a,b, 2016; Savoie et al., 2015; Xu H. et al., 2015; An et al., 2016; Huang et al., 2017; Li et al., 2017, 2018; Xiao et al., 2017; Zhang et al., 2017; Zhao F. et al., 2017; Zhang T. et al., 2018). With this strategy, more than 14% efficiencies have been obtained very recently (Xiao et al., 2017; Li et al., 2018).

Ternary blend polymer solar cells exhibit improved photocurrent generation compared to binary blend counterparts. This is simply due to additional absorption of the third material, which can expand the light-harvesting wavelength range. In some ternary blend polymer solar cells, the photocurrent is improved by the efficient energy transfer (Honda et al., 2009, 2010, 2011a; Xu et al., 2013; Lu et al., 2015a; Wang et al., 2015a, 2018a; Yang et al., 2017; Zhao F. et al., 2017). This is because excitons can be more efficiently harvested to donor/acceptor interfaces through the long-range energy transfer. In particular, this is more effective for highly crystalline polymers such as poly(3-hexylthiophene) (P3HT), because some excitons generated in large crystalline domains cannot arrive at donor/acceptor interfaces before deactivating to the ground state (Menke and Holmes, 2014; Wang et al., 2014a; Xu G. et al., 2015). For example, 10–20% excitons cannot arrive at donor/acceptor interfaces in blends of P3HT and [6,6]-phenyl-C_{61}-butyric acid methyl ester (PCBM). For the efficient energy transfer, it is required that the third material has a complementary absorption with a large absorption coefficient, which should overlap with the fluorescence spectrum of the other donor polymer. As such, it is worthy to develop organic semiconductors with a high optical absorption coefficient.

Herein, we synthesized a low-bandgap polymer, poly[*N*-9′-ethylhexyl-2,7-carbazole-*alt*-3,6-bis(bithiophen-5-yl)-2,5-diethylhexyl-2,5-dihydropyrrolo[3,4-]pyrrole-1,4-dione] (PCDPP4T). This polymer is based on diketopyrrolopyrrole (DPP) and carbazole (Cz) units, which are the same structure as the small conjugated molecule we reported previously: 3,6-bis{5′-(9-(2-ethylhexyl)-9*H*-carbazol-2-yl)-[2,2′-bithiophen]-5-yl}-2,5-bis(2-ethylhexyl)-pyrrolo[3,4-*c*]pyrole-1,4-dione (DPP4T-Cz) (Wang et al., 2018b). The absorption coefficient of the polymerized material PCDPP4T was slightly higher than that of DPP4T-Cz quadropolar small molecule. By using PCDPP4T as the third material into binary blends of P3HT and PCBM, the photocurrent was improved not only in the near-IR region but also in the visible region. As a result, the efficiency of ternary blend solar cells based on P3HT, PCBM, and PCDPP4T was increased by 30% compared with P3HT/PCBM binary blend devices. **Figure 1** shows the chemical structures of photovoltaic materials used in this study.

RESULTS AND DISCUSSION

Thermal Properties of PCDPP4T

The thermal stability of PCDPP4T was examined by thermogravimetric analysis (TGA) under nitrogen atmosphere. As shown in **Figure 2A**, PCDPP4T was thermally stable up to around 370 °C, which is an onset temperature of thermal decomposition, and then exhibited 5% weight loss at 430 °C. This thermal stability of PCDPP4T is enough to fabricate various optoelectronic devices. In addition, the phase transition characteristics of PCDPP4T was measured by differential scanning calorimetry (DSC). As shown in **Figure 2B**, PCDPP4T exhibited a melting peak at 233 °C and a crystalline peak at 183 °C, indicating that PCDPP4T is a crystalline polymer.

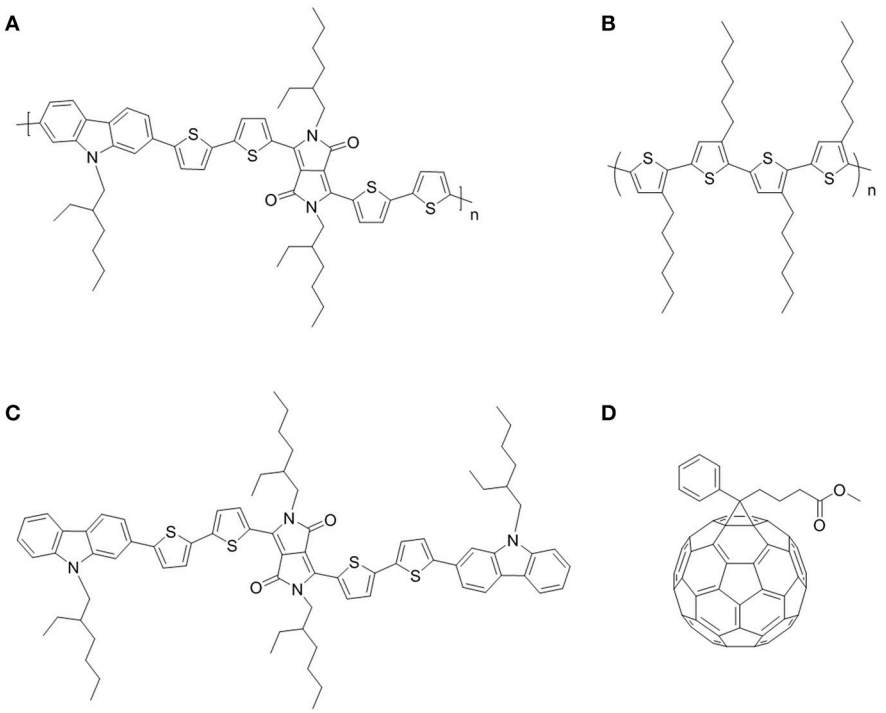

FIGURE 1 | Chemical structures of photovoltaic materials: PCDPP4T **(A)**, P3HT **(B)**, DPP4T-Cz **(C)**, and PCBM **(D)**.

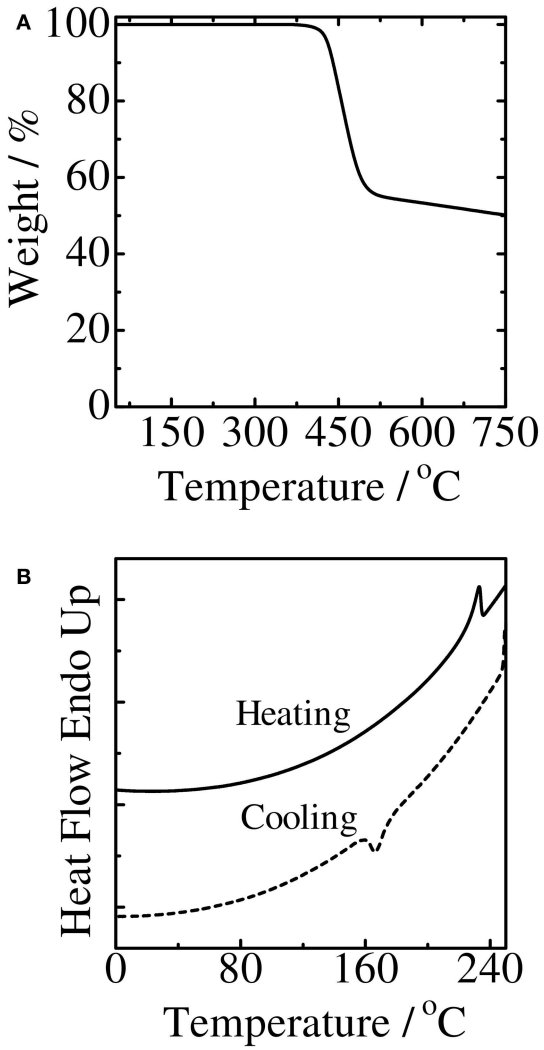

FIGURE 2 | Thermogravimetric analysis **(A)** and differential scanning calorimeter **(B)** curves of the polymers.

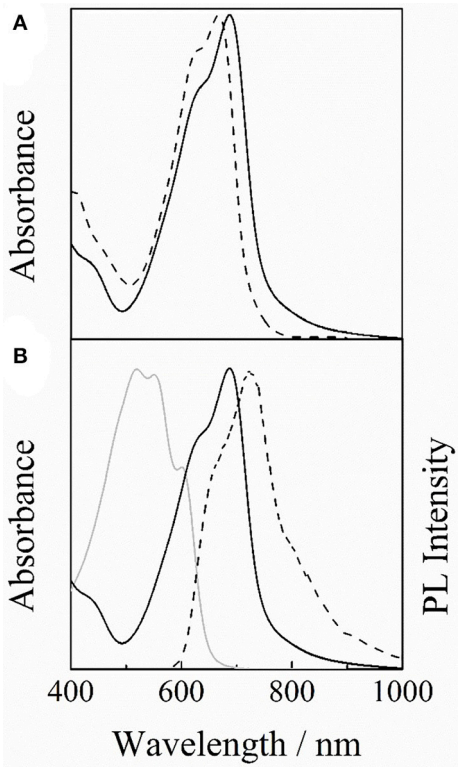

FIGURE 3 | (A) Absorption spectra of PCDPP4T in chloroform solution (broken line) and in solid film on a quartz substrate (solid line). **(B)** Absorption spectra of P3HT (gray solid line) and PCDPP4T (black solid line), and photoluminescence (PL) spectrum of P3HT (black broken line).

Optoelectronic Properties

As shown in **Figure 3A**, PCDPP4T exhibits a major absorption peak at around 665 nm with a shoulder at around 625 nm in solution. On the other hand, it exhibits a major absorption peak at around 685 nm in solid films. The absorption coefficient was as high as 1.3×10^5 cm^{-1} for PCDPP4T films, which is slightly larger than 1.0×10^5 cm^{-1} for DPP4T-Cz films. This large absorption coefficient is beneficial for energy transfer from wide-bandgap materials such as P3HT. The red-shifted absorption observed for PCDPP4T films indicates that PCDPP4T has longer effective conjugation lengths in solid states than in solutions. Furthermore, the absorption ratio of 0–0 to 0–1 bands was larger in solid films than in solutions. This is in contrast to the decrease in the absorption ratio of 0–0 to 0–1 bands observed for DPP4T-Cz molecules in solid states, suggesting formation of H-aggregates due to intermolecular π-π stacking. In other words, intrachain ordering is improved in PCDPP4T films while intermolecular π-π stacking is enhanced in DPP4T-Cz films.

As shown in **Figure 3B**, PCDPP4T exhibits a large absorption peak at around 685 nm and an absorption valley at around 500 nm while P3HT exhibits a large absorption band at around 550 nm. Because of the complementary relationship between these two absorption spectra, the absorption wavelength range can be extended from 400 to 950 nm by using PCDPP4T and P3HT polymers at the same time. Furthermore, the photoluminescence (PL) spectrum of P3HT has a substantial overlap with the absorption spectrum of PCDPP4T, which would result in the efficient energy transfer from P3HT to PCDPP4T. As reported previously (Wang et al., 2015a,b), this is beneficial for the efficient exciton harvesting to the donor/acceptor interface.

Figure 4 shows the highest occupied molecular orbital (HOMO) levels and the lowest unoccupied molecular orbital (LUMO) levels of the photoactive materials employed in this study. The HOMO level was evaluated by photoelectron yield spectroscopy (PYS) (see the **Supporting Information S1**) and the LUMO level was estimated from the optical bandgap and the HOMO level, as reported previously (Wang et al., 2014c). As shown in the figure, the HOMO and LUMO levels of PCDPP4T are evaluated to be −5.1 and −3.5 eV, respectively, which are located in between those of P3HT and PCBM. The cascaded energy structure with enough offset energy would be necessary

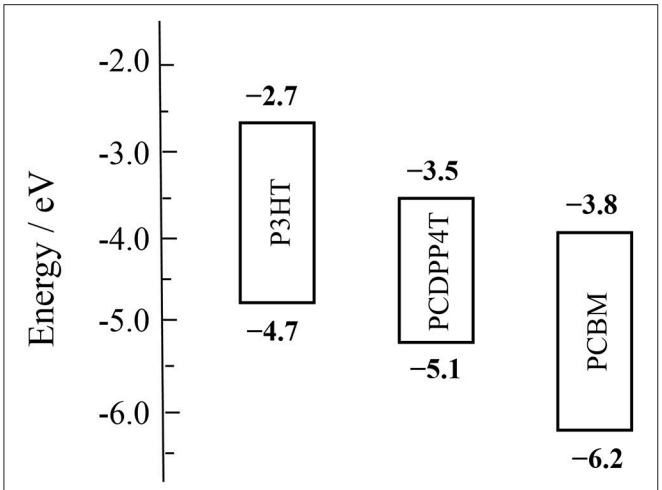

FIGURE 4 | HOMO and LUMO energy levels of materials employed in this study: P3HT, PCBM, and PCDPP4T.

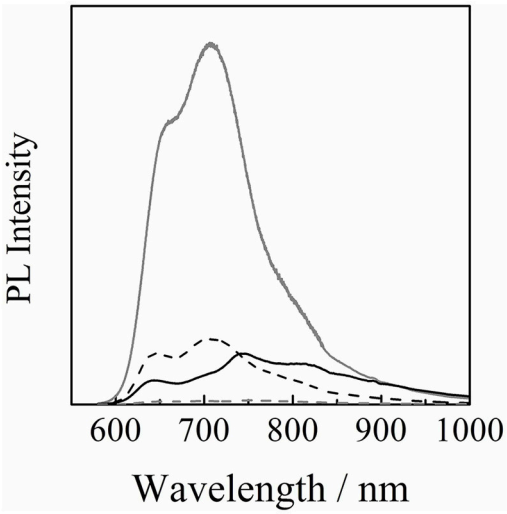

FIGURE 5 | PL spectra of P3HT neat (gray line) and blend films with different compositions: P3HT/PCBM (20 : 20, w/w) (black broken line), P3HT/PCBM/PCDPP4T (20 : 20 : 1.4, w/w/w) (gray broken line), and P3HT/PCDPP4T (3 : 4, w/w) (black solid line) blend films. The PL intensity of P3HT was corrected for variation in the absorption at an excitation wavelength of 500 nm. The PL intensity of PCDPP4T was corrected by subtracting the PL intensity due to the direct excitation of PCDPP4T at 500 nm.

for the efficient charge transfer at the interfaces of P3HT/PCBM, PCDPP4T/PCBM, and P3HT/PCDPP4T.

Energy Transfer and Photoluminescence Quenching

In order to discuss the energy transfer from P3HT to PCDPP4T, we evaluated the Förster radius by the equation 1 with the same parameters as reported previously (Wang et al., 2018b).

$$R_0{}^6 = \frac{9000\kappa^2(\ln 10)\eta_D}{128\pi^5 n^4 N_A}\int f_D(\tilde{\nu})\varepsilon_A(\tilde{\nu})\frac{d\tilde{\nu}}{\tilde{\nu}^4} \quad (1)$$

On the basis of the equation 1, a Förster radius was evaluated to be 4.0 nm for P3HT and PCDPP4T, which is longer than 3.5 nm evaluated for P3HT and DPP4T-Cz. The increased Förster radius, which is due to the increased absorption coefficient of PCDPP4T, would be beneficial for the efficient exciton harvesting by the energy transfer as will be mentioned below.

As shown in **Figure 5**, the PL intensity from P3HT was completely quenched for the P3HT/PCBM/PCDPP4T ternary blend while the PL intensity was quenched for the P3HT/PCBM binary blend down to ∼20% relative to that of a P3HT neat film. This is probably because 20% of P3HT excitons that would be lost in the absence of PCDPP4T are harvested to PCDPP4T domains by the energy transfer and then quenched by the charge transfer to PCBM. Indeed, for a P3HT/PCDPP4T binary blend film, the PL intensity of P3HT decreased obviously and instead the PL intensity of PCDPP4T was observed in the near-IR region even though P3HT was selectively excited. This finding indicates that there is the efficient energy transfer from P3HT to PCDPP4T. In summary, the energy transfer from P3HT to PCDPP4T plays an important role in the exciton harvesting to donor/acceptor interfaces. As a result, the PL quenching efficiency increased from 80% for the P3HT/PCBM binary blend to 100% for the P3HT/PCBM/PCDPP4T ternary blend.

Photovoltaic Properties

Figure 6A shows the J–V characteristics of the binary blend and ternary blend solar cells under simulated solar illumination (AM1.5G) with an intensity of 100 mA cm^{-2}. As shown in the figure, the J_{SC} was improved from 9.4 to 11.1 mA cm^{-2} by loading of only 3.4 wt% of PCDPP4T into P3HT/PCBM binary blends. On the other hand, no distinct change was found for the open-circuit voltage (V_{OC}). This finding indicates that the charge recombination is still dominant between P3HT polarons and PCBM anions in the ternary blend solar cells. This is because most of P3HT domains still contact with PCBM domains at such a small fraction of PCDPP4T. Interestingly, the fill factor (FF) slightly increased from 0.55 for P3HT/PCBM binary blends to 0.59 for P3HT/PCBM/PCDPP4T ternary blends. The improved FF is consistent with the decrease in series resistance (R_s) and the increase in parallel resistance (R_p) with increasing low-bandgap polymer PCDPP4T as shown in **Table 1**. The decreased R_s is probably ascribed to less charge trap sites due to a reduced intermolecular π-π stacking observed in the absorption spectrum. Such improvements in FF have also been reported for other ternary blend polymer solar cells (Gasparini et al., 2016; Lee et al., 2017; Zhang et al., 2017; Zhao F. et al., 2017; Wang et al., 2018a), suggesting that charge transport might be improved in ternary blends. This is consistent with a slightly improved hole mobility observed for ternary blend films even with a similar surface morphology in comparison with those of binary blend films (see the **Supporting Informations S2**, **S3**). As a result, the power conversion efficiency (PCE) was improved from 2.7% for

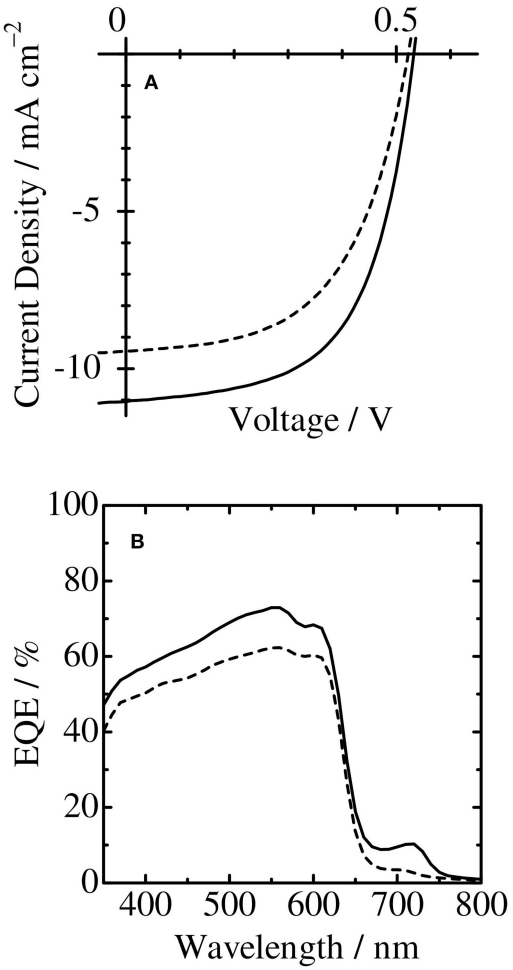

FIGURE 6 | (A) *J–V* characteristics and **(B)** external quantum efficiency (EQE) of P3HT/PCBM binary blend (broken line) and P3HT/PCBM/PCDPP4T ternary blend (solid line) solar cells under AM1.5G simulated solar illumination.

the binary blend solar cell to 3.5% for the ternary blend solar cell. Further addition of PCDPP4T rather decreased the photocurrent and hence degraded the overall PCE as shown in **Table 1**. This is probably because additional PCDPP4T would be located in P3HT or PCBM domains rather than at the P3HT/PCBM interface where desirable cascaded energy structure can be formed.

In order to discuss the improved J_{SC}, we measured the external quantum efficiency (EQE) spectra of the binary and ternary blend polymer solar cells. The J_{SC}^{calc} calculated from the EQE and solar spectra is in good agreement with the J_{SC} directly measured from the *J–V* curve as shown in **Table 1**. With the loading of 3.4 wt% PCDPP4T into the binary blend, an additional EQE signal was found in the near-IR region for the ternary blend, which is ascribed to the PCDPP4T absorption. Interestingly, as shown in **Figure 6B**, the EQE signal due to the P3HT absorption was also enhanced in the visible region at around 550 nm from 62 to 73%, although no difference in the absorption was found between P3HT/PCBM binary and P3HT/PCBM/PCDPP4T ternary blend films. As reported previously, (Honda et al., 2011b; Tamai et al., 2015; Wang et al., 2015b) the increased EQE is mainly because P3HT singlet excitons are more efficiently harvested to an interface of P3HT and PCBM by the energy transfer from P3HT to PCDPP4T followed by charge dissociation. This is consistent with larger PL quenching efficiency observed for the ternary blend as mentioned above. In other words, there are two mechanisms for the increase in the J_{SC}: one is the photocurrent by additional light harvesting at the PCDPP4T absorption band in the near-IR region, and the other is the photocurrent by the efficient exciton harvesting from P3HT to PCDPP4T. The increase in the J_{SC} was estimated to be 0.6 mA cm^{-2} for the additional light harvesting and 1.1 mA cm^{-2} for the exciton harvesting due to the energy transfer. In other words, the energy transfer from P3HT to PCDPP4T plays a dominant role in the improvement in the J_{SC}.

Finally, we consider the future direction for highly efficient ternary blend polymer solar cells by comparing P3HT/PCBM/PCDPP4T polymer-based ternary blend solar cells with P3HT/PCBM/DPP4T-Cz small molecule-based ternary blend solar cells reported previously (Wang et al., 2018b). First, the absorption coefficient is improved for the low-bandgap polymer PCDPP4T compared to that of conjugated small molecule DPP4T-Cz. This would be due to the longer effective conjugation in polymer chains. However, the improvement in J_{SC} for polymer-based ternary blends is limited to <20%, which is less than that observed for small molecule-based ternary blends. In addition, the improvement in V_{OC} for polymer-based ternary blends is also less than that observed for small molecule-based ternary blends. As a result, the overall PCE for polymer-based ternary cells is lower than that for small molecule-based ternary cells. This is probably due to a poor compatibility between P3HT and PCDPP4T because both polymers are crystalline materials. On the other hand, the improvement in FF for polymer-based ternary blends is higher than that observed for small molecule-based ternary blends. This might be due to reduced trap sites in ternary blends. We therefore suggest that low-bandgap amorphous polymers would be more suitable for highly efficient ternary blend polymer solar cells.

CONCLUSIONS

We have synthesized a low-bandgap conjugated polymer PCDPP4T incorporating diketopyrrolopyrrole and carbazole unit in the main chain. The absorption coefficient was as high as of the order of 10^5 cm^{-1}, which is slightly higher than that of DPP4T-Cz monomer unit molecules. The absorption spectrum indicates that intrachain ordering is improved in solid states rather than interchain π-π stacking, which would reduce trap sites and hence result in an efficient charge transport. Because of the large absorption coefficient, the PCE is improved by 30% for ternary solar cells with only 3.4 wt% of PCDPP4T. This is mainly due to the increased photocurrent not only in the near-IR range but also in the visible range. In other words, there are two mechanisms for the photocurrent improvement: one is due to the improved lighting harvesting by PCDPP4T absorption in the near-IR region and the other is due to the improved

TABLE 1 | Photovoltaic parameters of binary and ternary blend solar cells.

P3HT : PCBM : PCDPP4T	J_{SC} mA cm^{-2}	J_{SC}^{calc} mA cm^{-2}	V_{OC} V	FF	PCE %	R_s Ω cm^2	R_p kΩ cm^2
20 : 20 : 0 (0 wt%)	9.4	9.2	0.52	0.55	2.7	2.1	600
20 : 20 : 0.7 (1.7 wt%)	10.7	10.3	0.52	0.57	3.2	2.0	800
20 : 20 : 1.4 (3.4 wt%)	11.1	10.6	0.53	0.59	3.5	1.0	890
20 : 20 : 2.1 (5.0 wt%)	10.3	9.9	0.53	0.56	3.0	1.2	850

exciton harvesting by energy transfer from P3HT to PCDPP4T. Further addition of PCDPP4T might disturb blend morphologies and hence degraded photovoltaic performances. We therefore conclude that the compatibility between two donor polymers plays an important role in the photovoltaic performances of ternary blend solar cells. We thus propose that the photovoltaic performances would be further improved by using a combination of a crystalline wide-bandgap polymer and an amorphous low-bandgap polymer with a high absorption coefficient.

EXPERIMENTAL SECTION

Materials

Poly(3-hexylthiophene) (regioregular P3HT, M_w = 50,000), zinc acetate dehydrate ($Zn(CH_3COO)_2{\cdot}2H_2O$), ethanolamine ($NH_2CH_2CH_2OH$), 2-methoxyethanol ($CH_3OCH_2CH_2OH$) were purchased from Sigma-Aldrich. A fullerene acceptor was purchased from Frontier Carbon (PCBM, E100H). 2,7-Dibromocarbazole (Cz-2Br), 1-bromo-2-ethylhexane, tri(*o*-tolyl)phosphine (P(*o*-tol)$_3$), and tris(dibenzylideneacetone) dipalladium(0) ($Pd_2(dba)_3$) were purchased from Tokyo Chemical Industry. All materials were used without further purification.

Synthesis

A low-bandgap polymer PCDPP4T was synthesized as reported previously (Wang et al., 2018b) and the synthetic routes are shown in **Scheme 1**. A monomer M2 was synthesized from 2,7-dibromocarbazole (Cz-2Br) and 1-bromo-2-ethylhexane through the Hofmann alkylation reaction. The PCDPP4T polymer was prepared from M2 and DPP4T through the Stille coupling reaction. The structures of the monomer and the polymer have been confirmed by ^{1}H NMR.

Synthesis of M2

To a solution of 1 g (3.07 mmol) of 2,7-dibromocarbazole (Cz-2Br) in 12 mL of acetone, 368.3 mg (6.14 mmol) of potassium hydroxide powder, 1.2 mL (6.14 mmol) of 2-ethylhexyl bromide, and 0.1 g (0.29 mmol) of tetrabutylammonium hydrogen sulfate as phase-transfer catalyst were added. The mixture was heated to reflux for 24 h, and then extracted with dichloromethane. The organic layer was washed with water and dried over anhydrous magnesium sulfate. The crude product was performed by column chromatography on silica gel with ethyl acetate: petroleum ether (1 : 5, v/v) as an eluent, yielding 1.2 g (88%) of 2,7-dibromo-9-(2-ethylpentyl)-9*H*-carbazole (M2) as colorless oil. ^{1}H-NMR (400 MHz, $CDCl_3$, δ): 7.94 (2H, d), 7.52 (2H, d), 7.38 (2H, dd), 4.10 (2H, m), 1.51–1.20 (8H, m), 1.01–0.82 (6H, m).

Synthesis of PCDPP4T

First, DPP4T (350 mg, 0.34 mmol), M2 (148 mg, 0.34 mmol), and (P(*o*-tol)$_3$) (12.4 mg, 0.0406 mmol) were dissolved in 15 mL anhydrous toluene. Then, the solution was purged with argon for 30 min, and $Pd_2(dba)_3$ (18.7 mg, 0.0204 mmol) was added. The reaction mixture was heated slowly to reflux for 72 h. After the reaction was completed, 2-bromothiophene (0.15 equiv.) was added to the reaction solution. After 5 h, 2-tributylstannyl thiophene (0.15 equiv.) was added and the reaction continued for another 12 h to complete the end-capping reaction. The reaction solution was cooled to room temperature, and then KF (2.7 g in 5 mL of water) was added and stirred for 6 h to remove the tin impurity. The chloroform solution containing the polymer was precipitated into 300 mL of methanol/water (15 : 1, v/v), and then the crude product was extracted with methanol and hexanes in a Soxhlet apparatus to remove the oligomers and catalyst residues until the extraction solution was colorless. Finally the crude solid was extracted with chloroform. The chloroform fraction was condensed to about 10 mL under reduced pressure and precipitated in 500 mL of methanol/water (15 : 1, v/v), filtered through 0.45 μm Nylon filter and dried under vacuum at 40 °C for 6 h, yielding 283 mg (85%) of PCDPP4T as dark green solid. ^{1}H-NMR (400 MHz, $CDCl_3$, δ): 8.95 (d, 2H), 7.76–7.72 (m, 4H), 7.57–7.52 (m, 4H), 7.32–7.25 (m, 2H), 7.20–7.14 (m,2H), 4.30 (t, 4H), 4.21(m, 2H), 2.03 (m, 3H), 1.80–1.50 (m, 8H), 1.50–1.15 (m, 24H), 1.06–0.80 (m, 10H). The number average molecular weight (M_n): 28 000, polydispersity index (PDI): 4.7.

Materials Characterization

The chemical structure of M2 and PCDPP4T was confirmed by NMR spectra, which was acquired at room temperature with a 400-MHz NMR spectrometer (Bruker, Avance III) in deuterochloroform containing tetramethylsilane as an internal reference. Absorption and PL spectra were measured using a spectrophotometer (Hitachi, U-4100) and a spectrofluorometer (Horiba Jobin Yvon, NanoLog) that was equipped with a calibrated imaging detector (Horiba Jobin Yvon, iHR320), respectively. The ionization potential of the polymers was measured with a PYS (Riken Keiki, AC-3). The samples were fabricated by spin-coating from stock solution onto a cleaned ITO substrate. The threshold energy for the photoelectron emission was estimated on the basis of the cubic root of the photoelectron yield plotted against the incident photon energy. The average molecular weight and polydispersity index (PDI) of PCDPP4T were measured by gel permeation chromatography (GPC) analysis (Waters, 1515) with THF as an eluent and polystyrene as a standard. Thermal stability of the sample was evaluated with Perkin-Elmer TGA 4000. About 5 mg of sample

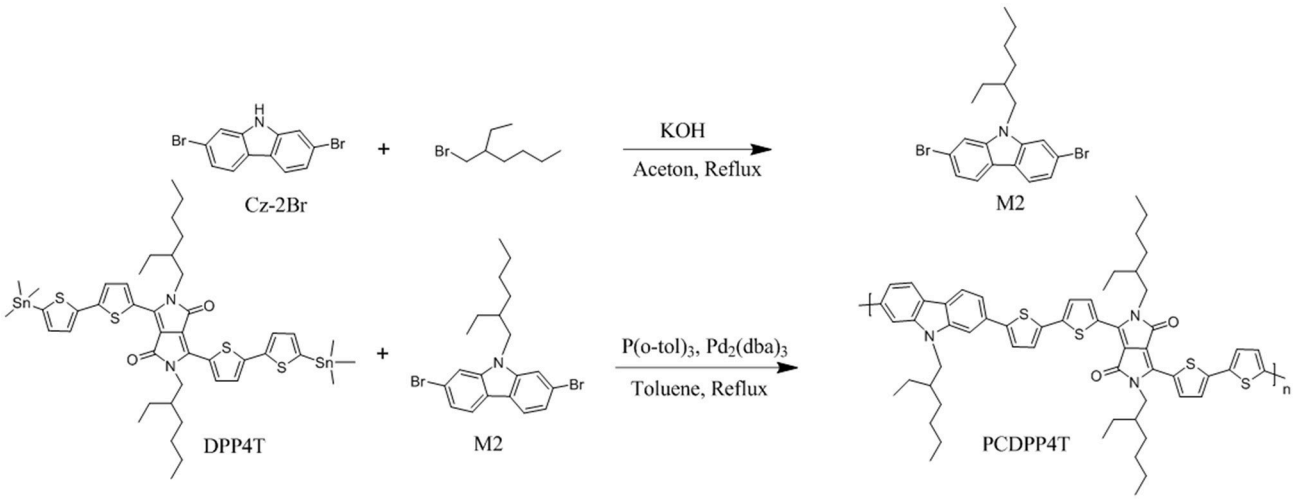

SCHEME 1 | Synthetic route of PCDPP4T.

was placed in the pan and heated from 35 to 700 °C at a heating rate of 10 °C min^{-1} under a nitrogen atmosphere. The phase transition behavior of PCDPP4T was measured by differential scanning calorimetry (Perkin-Elmer DSC 8000) using about 5 mg of sample under a nitrogen atmosphere at a flow rate of 50 mL min^{-1}. The instrument was calibrated for both heat flow and temperature using indium and zinc standards. When tested, samples were heated to 300 °C at a heating rate of 10 °C min^{-1}, and cooled to 40 °C at a cooling rate of 10 °C min^{-1}. The thermogram was recorded from the DSC first heating and cooling round.

Device Fabrication and Characterization

The indium–tin-oxide (ITO)-coated glass substrates were washed by ultrasonication in toluene, acetone, and ethanol for 15 min in sequence, dried with N_2, and then cleaned with UV–ozone cleaner for 30 min. A transparent nano-particle ZnO thin film, which was employed as an electron-transporting layer, was spin-coated from a ZnO precursor on the ITO-glass substrate at 800 rpm for 10 s and 3,000 rpm for 60 s in sequence, and then were anneal at 180 °C for 1 h in air, during this process the precursor was converted to solid-state ZnO. The ZnO precursor solution was prepared by dissolving $Zn(CH_3COO)_2{\cdot}2H_2O$ (1 g) and $NH_2CH_2CH_2OH$ (0.28 g) in $CH_3OCH_2CH_2OH$ (15 mL) under vigorous stirring for one night for the hydrolysis reaction in air. Subsequently, a ternary blend active layer of P3HT/PCBM/PCDPP4T was spin-coated at a spin rate of 600 rpm for 60 s. The ternary blend solution was prepared as follows: P3HT, PCBM, and PCDPP4T were dissolved in *o*-dichlorobenzene at a concentration ratio of 20 : 20 : 1.4 mg mL^{-1} ([PCDPP4T] = 3.4 wt%) and then the mixed solution was stirred at 60 °C overnight. Note that the weight fraction of the low-bandgap polymer PCDPP4T was optimized in the range from 2.4 to 4.8 wt%. Finally, a hole collection electrode of 10-nm-thick MoO_3 and 100-nm-thick Au was thermally evaporated under vacuum at a pressure of 3×10^{-4} Pa. The effective device area was 0.07 cm^2.

J–V characteristics were measured with a direct current (DC) voltage and current source/monitor (Keithley, 2611B) in the dark and under the illumination with AM 1.5G simulated solar light with 100 mW cm^{-2}. The light intensity was corrected with a calibrated silicon photodiode reference cell (Bunkoh-Keiki, BS-520). The EQE spectra were measured with a spectral response measurement system (Bunko-Keiki Co., ECT-250D). The power of the incident monochromatic light was kept under 0.05 mW cm^{-2}, which was measured with a calibrated silicon reference cell (Bunkoh-Keiki, BS-520BK).

AUTHOR CONTRIBUTIONS

YW, BW, HK, and HO designed the research objective. JC and RI conducted field experiments. YW performed statistical analysis and drafted the initial article. YW, HK, and HO contributed section content and edited to subsequent drafts, while all authors reviewed and provided feedstock on the submitted article.

FUNDING

This work was partly supported by the Natural Science Foundation of Jiangsu Province (BK20160280), Double Plan of Jiangsu Province, and JST ALCA Grant Number JPMJAL1404, Japan.

SUPPLEMENTARY MATERIAL

The Supplementary Material for this article can be found online at: https://www.frontiersin.org/articles/10.3389/fenrg.2018.00113/full#supplementary-material

REFERENCES

Ameri, T., Khoram, P., Min, J., and Brabec, C. J. (2013). Organic ternary solar cells: a review. *Adv. Mater.* 25, 4245–4266. doi: 10.1002/adma.201300623

Ameri, T., Min, J., Li, N., Machui, F., Baran, D., Forster, M., et al. (2012). Performance enhancement of the P3HT/PCBM solar cells through NIR sensitization using a small-bandgap polymer. *Adv. Energy Mater.* 2, 1198–1202. doi: 10.1002/aenm.201200219

An, Q., Zhang, F., Zhang, J., Tang, W., Deng, Z., and Hu, B. (2016). Versatile ternary organic solar cells: a critical review. *Energy Environ. Sci.* 9, 281–322. doi: 10.1039/C5EE02641E

Bin, H., Zhang, Z., Gao, L., Chen, S., Zhong, L., Xue, L., et al. (2016). Non-fullerene polymer solar cells based on alkylthio and fluorine substituted 2d-conjugated polymers reach 9.5% efficiency. *J. Am. Chem. Soc.* 138, 4657–4664. doi: 10.1021/jacs.6b01744

Dou, L., You, J., Yang, J., Chen, C., He, Y., Murase, S., et al. (2011). Tandem polymer solar cells featuring a spectrally matched low-bandgap polymer. *Nat. Photonics* 6, 180–185. doi: 10.1038/nphoton.2011.356

Gasparini, N., Jiao, X. C., Heumueller, T., Baran, D., Matt, G. J., Fladischer, S., et al. (2016). Designing ternary blend bulk heterojunction solar cells with reduced carrier recombination and a fill factor of 77%. *Nat. Energy* 1, 16118–16126. doi: 10.1038/nenergy.2016.118

Halls, J. J. M., Walsh, C. A., Greenham, N. C., Marseglia, E. A., Friend, R. H., Moratti, S. C., et al. (1995). Efficient photodiodes from interpenetrating polymer networks. *Nature* 376, 498–500. doi: 10.1038/376498a0

Honda, S., Nogami, T., Ohkita, H., Benten, H., and Ito, S. (2009). Improvement of the light-harvesting efficiency in polymer/fullerene bulk heterojunction solar cells by interfacial dye modification. *ACS Appl. Mater. Interfaces* 1, 804–810. doi: 10.1021/am800229p

Honda, S., Ohkita, H., Benten, H., and Ito, S. (2010). Multi-colored dye sensitization of polymer/fullerene bulk heterojunction solar cells. *Chem. Commun.* 46, 6596–6598. doi: 10.1039/c0cc01787f

Honda, S., Ohkita, H., Benten, H., and Ito, S. (2011a). Selective dye loading at the heterojunction in polymer/ fullerene solar cells. *Adv. Energy Mater.* 1, 588–598. doi: 10.1002/aenm.201100094

Honda, S., Yokoya, S., Ohkita, H., Benten, H., and Ito, S. (2011b). Light-harvesting mechanism in polymer/fullerene/dye ternary blends studied by transient absorption spectroscopy. *J. Phys. Chem. C* 115, 11306–11317. doi: 10.1021/jp201742v

Huang, H., Yang, L., and Sharma, B. (2017). Recent advances in organic ternary solar cells. *J. Mater. Chem. A* 5, 9418–9420. doi: 10.1039/C7TA90087B

Kim, Y., Cook, S., Tuladhar, S. M., Choulis, S. A., Nelson, J., Durrant, J. R., et al. (2006). A strong regioregularity effect in self-organizing conjugated polymer films and high-efficiency polythiophene: fullerene solar cells. *Nat. Mat.* 5, 197–203. doi: 10.1038/nmat1574

Lee, J., Tamilavan, V., Rho, K. H., Keum, S., Park, K. H., Han, D., et al. (2017). Overcoming fill factor reduction in ternary polymer solar cells by matching the highest occupied molecular orbital energy levels of donor polymers. *Adv. Energy Mater.* 8:1702251. doi: 10.1002/aenm.201702251

Li, G., Shrotriya, V., Huang, J. S., Yao, Y., Moriarty, T., Emery, K., et al. (2005). High-efficiency solution processable polymer photovoltaic cells by self-organization of polymer blends. *Nat. Mater.* 4, 864–868. doi: 10.1038/nmat1500

Li, H., Lu, K., and Wei, Z. (2017). Polymer/small molecule/fullerene based ternary solar cells. *Adv. Energy Mater.* 7:1602540. doi: 10.1002/aenm.201602540

Li, H., Xiao, Z., Ding, L., and Wang, J. (2018). Thermostable single-junction organic solar cells with a power conversion efficiency of 14.62%. *Sci. Bull.* 63, 340–342. doi: 10.1016/j.scib.2018.02.015

Li, S., Ye, L., Zhao, W., Zhang, S., Mukherjee, S., Ade, H., et al. (2016). Energy-level modulation of small-molecule electron acceptors to achieve over 12% efficiency in polymer solar cells. *Adv. Mater.* 28, 9423–9429. doi: 10.1002/adma.201602776

Liang, Y., Xu, Z., Xia, J., Tsai, S. T., Wu, Y., Li, G., et al. (2010). For the bright future-bulk heterojunction polymer solar cells with power conversion efficiency of 7.4%. *Adv. Mater.* 22, E135–E138. doi: 10.1002/adma.200903528

Liu, Y., Zhao, J., Li, Z., Mu, C., Ma, W., Hu, H., et al. (2014). Aggregation and morphology control enables multiple cases of high-efficiency polymer solar cells. *Nat. Commun.* 5:5293. doi: 10.1038/ncomms6293

Lu, H., Xu, X., and Bo, Z. (2016). Perspective of a new trend in organic photovoltaic: ternary blend polymer solar cells. *Sci. China Mater.* 59, 444–458. doi: 10.1007/s40843-016-5069-6

Lu, L., Chen, W., Xu, T., and Yu, L. (2015a). High-performance ternary blend polymer solar cells involving both energy transfer and hole relay processes. *Nat. Commun.* 6:7327. doi: 10.1038/ncomms8327

Lu, L., Kelly, M. A., You, W., and Yu, L. (2015b). Status and prospects for ternary organic photovoltaics. *Nat. Photon.* 9, 491–500. doi: 10.1038/nphoton.2015.128

Menke, S. M., and Holmes, R. J. (2014). Exciton diffusion in organic photovoltaic cells. *Energy Environ. Sci.* 7, 499–512. doi: 10.1039/C3EE42444H

Padinger, F., Rittberger, R. S., and Sariciftci, N. S. (2003). Effects of postproduction treatment on plastic solar cells. *Adv. Funct. Mater.* 13, 85–88. doi: 10.1002/adfm.200390011

Peet, J., Kim, J. Y., Coates, N. E., Ma, W. L., Moses, D., Heeger, A. J., et al. (2007). Efficiency enhancement in low-bandgap polymer solar cells by processing with alkane dithiols. *Nat. Mater.* 6, 497–500. doi: 10.1038/nmat1928

Peet, J., Tamayo, A. B., Dang, X. D., Seo, J. H., and Nguyen, T. Q. (2008). Small molecule sensitizers for near-infrared absorption in polymer bulk heterojunction solar cells. *Appl. Phys. Lett.* 93:163306. doi: 10.1063/1.3001802

Savoie, B. M., Dunaisky, S., Marks, T. J., and Ratner, M. A. (2015). The scope and limitations of ternary blend organic photovoltaics. *Adv. Energy Mater.* 5:1400891. doi: 10.1002/aenm.201400891

Shaheen, S. E., Brabec, C. J., Sariciftci, N. S., Padinger, F., Fromherz, T., and Hummelen, J. C. (2001). 2.5% efficient organic plastic solar cells. *Appl. Phys. Lett.* 78, 841–843. doi: 10.1063/1.1345834

Sun, J., Ma, X., Zhang, Z., Yu, J., Zhou, J., Yin, X., et al. (2018). Dithieno[3,2-b:2′,3′-d]pyrrol fused nonfullerene acceptors enabling over 13% efficiency for organic solar cells. *Adv. Mater.* 30:e1707150. doi: 10.1002/adma.201707150

Tamai, Y., Ohkita, H., Benten, H., and Ito, S. (2015). Exciton diffusion in conjugated polymers: from fundamental understanding to improvement in photovoltaic conversion efficiency. *J. Phys. Chem. Lett.* 6, 3417–3428. doi: 10.1021/acs.jpclett.5b01147

Vohra, V., Kawashima, K., Kakara, T., Koganezawa, T., Osaka, I., Takimiya, K., et al. (2015). Efficient inverted polymer solar cells employing favourable molecular orientation. *Nat. Photonics* 9, 403–408. doi: 10.1038/nphoton.2015.84

Wang, Y., Benten, H., Ohara, S., Kawamura, D., Ohkita, H., and Ito, S. (2014a). Measurement of exciton diffusion in a well-defined donor/acceptor heterojunction based on a conjugated polymer and cross-linked fullerene derivative. *ACS Appl. Mater. Interfaces* 6, 14108–14115. doi: 10.1021/am503434p

Wang, Y., Kim, D. K., Wang, B., and Ohkita, H. (2018a). Visible sensitization for non-fullerene polymer solar cells using a wide bandgap polymer. *J. Photopolym. Sci. Technol.* 31, 177–181. doi: 10.2494/photopolymer.31.177

Wang, Y., Ohkita, H., Benten, H., and Ito, S. (2014b). Near-IR sensitization of polymer solar cells incorporating low-bandgap small molecule. *Trans. Mat. Res. Soc. Japan* 39, 439–442. doi: 10.14723/tmrsj.39.439

Wang, Y., Ohkita, H., Benten, H., and Ito, S. (2015a). Highly efficient exciton harvesting and charge transport in ternary blend solar cells based on wide- and low-bandgap polymers. *Phys. Chem. Chem. Phys.* 17, 27217–27224. doi: 10.1039/C5CP05161D

Wang, Y., Ohkita, H., Benten, H., and Ito, S. (2015b). Efficient exciton harvesting through long-range energy transfer. *ChemPhysChem* 16, 1263–1267. doi: 10.1002/cphc.201402740

Wang, Y., Wang, T., Chen, J., Kim, H. D., Gao, P., Wang, B., et al. (2018b). Quadrupolar D-A-D diketopyrrolopyrrole-based small molecule for ternary blend polymer solar cells. *Dyes Pigments* 158, 213–218. doi: 10.1016/j.dyepig.2018.05.048

Wang, Y., Zheng, B., Tamai, Y., Ohkita, H., Benten, H., and Ito, S. (2014c). Dye sensitization in the visible region for low-bandgap polymer solar cells. *J. Electrochem. Soc.* 161, D3093–D3096. doi: 10.1149/2.015407jes

Xiao, Z., Jia, X., and Ding, L. (2017). Ternary organic solar cells offer 14% power conversion efficiency. *Sci. Bull.* 62, 1562–1564. doi: 10.1016/j.scib.2017.11.003

Xu, G., Lu, N., Wang, W., Gao, N., Ji, Z., Li, L., et al. (2015). Universal description of exciton diffusion length in organic photovoltaic cell. *Org. Electron.* 23, 53–56. doi: 10.1016/j.orgel.2015.04.006

Xu, H., Ohkita, H., Tamai, Y., Benten, H., and Ito, S. (2015). Interface engineering for ternary blend polymer solar cells with a heterostructured near-IR dye. *Adv. Mater.* 27, 5868–5874. doi: 10.1002/adma.201502773

Xu, H., Wada, T., Ohkita, H., Benten, H., and Ito, S. (2013). Dye sensitization of polymer/fullerene solar cells incorporating bulky phthalocyanines. *Electrochim. Acta* 100, 214–219. doi: 10.1016/j.electacta.2012.05.155

Xu, X., Yu, T., Bi, Z., Ma, W., Li, Y., and Peng, Q. (2018). Realizing over 13% efficiency in green-solvent-processed nonfullerene organic solar cells enabled by 1,3,4-thiadiazole-based wide-bandgap copolymers. *Adv. Mater.* 30:1703973. doi: 10.1002/adma.201703973

Yang, L., Gu, W., Hong, L., Mi, Y., Liu, F., Liu, M., et al. (2017). High performing ternary solar cells through Förster resonance energy transfer between nonfullerene acceptors. *ACS Appl. Mater. Interfaces* 9, 26928–26936. doi: 10.1021/acsami.7b08146

Yang, L., Yan, L., and You, W. (2013). Organic solar cells beyond one pair of donor-acceptor: ternary blends and more. *J. Phys. Chem. Lett.* 4, 1802–1810. doi: 10.1021/jz400723u

Yang, Y., Chen, W., Dou, L., Chang, W., Duan, H., Bob, B., et al. (2015). High-performance multiple-donor bulk heterojunction solar cells. *Nat. Photonics* 9, 190–198. doi: 10.1038/nphoton.2015.9

Yu, G., Gao, J., Hummelen, J. C., Wudl, F., and Heeger, A. J. (1995). Polymer photovoltaic cells: enhanced efficiencies via a network of internal donor-acceptor heterojunctions. *Science* 270, 1789–1791. doi: 10.1126/science.270.5243.1789

Zhang, G., Zhang, K., Yin, Q., Jiang, X., Wang, Z., Xin, J., et al. (2017). High-performance ternary organic solar cell enabled by a thick active layer containing a liquid crystalline small molecule donor. *J. Am. Chem. Soc.* 139, 2387–2395. doi: 10.1021/jacs.6b11991

Zhang, S., Qin, Y., Zhu, J., and Hou, J. (2018). Over 14% efficiency in polymer solar cells enabled by a chlorinated polymer. *Adv. Mater.* 30:1800868. doi: 10.1002/adma.201800868

Zhang, T., Zhao, X. L., Yang, D. L., Tian, Y. M., and Yang, X. N. (2018). Ternary organic solar cells with > 11% efficiency incorporating thick photoactive layer and nonfullerene small molecule acceptor. *Adv. Energy Mat.* 8:1701691. doi: 10.1002/aenm.201701691

Zhao, F., Li, Y., Wang, Z., Yang, Y., Wang, Z., He, G., et al. (2017). Combining energy transfer and optimized morphology for highly efficient ternary polymer solar cells. *Adv. Energy Mater.* 7:1602552. doi: 10.1002/aenm.201602552

Zhao, W., Li, S., Yao, H., Zhang, S., Zhang, Y., Yang, B., et al. (2017). Molecular optimization enables over 13% efficiency in organic solar cells. *J. Am. Chem. Soc.* 139, 7148–7151. doi: 10.1021/jacs.7b02677

Conflict of Interest Statement: The authors declare that the research was conducted in the absence of any commercial or financial relationships that could be construed as a potential conflict of interest.